Project "FEUERDRACHE": Process development and control of contact firing processes for high-efficiency silicon solar cells

Cite as: AIP Conference Proceedings **2367**, 020004 (2021); https://doi.org/10.1063/5.0056036
Published Online: 01 June 2021

G. Emanuel, D. Ourinson, G. Dammaß, H. Müller, C. Sternkiker, F. Ogiewa, K. Rahmanpour, T. Javaid, A. Csordás, S. Nold, S. W. Glunz, and F. Clement

Project "FEUERDRACHE": Process Development and Control of Contact Firing Processes for High-efficiency Silicon Solar Cells

G. Emanuel[1,a], D. Ourinson[1], G. Dammaß[2], H. Müller[3], C. Sternkiker[4], F. Ogiewa[5], K. Rahmanpour[1], T. Javaid[1], A. Csordás[1], S. Nold[1], S. W. Glunz[1], F. Clement[1]

[1]Fraunhofer ISE, Heidenhofstraße 2, 79110 Freiburg, Germany
[2] InfraTec GmbH, Gostritzer Straße 61-63, 01217 Dresden, Germany
[3] Rehm Thermal Systems GmbH, Leinenstraße 7, 89143 Blaubeuren-Seissen, Germany
[4] Former: Heraeus Noblelight GmbH, Reinhard-Heraeus-Ring 7, 63801 Kleinostheim, Germany
[5] Trumpf Photonic Components GmbH, Campus-Boulevard 79, 52074 Aachen

[a)]Corresponding author: gernot.emanuel@ise.fraunhofer.de

Abstract. Being a key technology in silicon solar cell production, the firing process conducted in infrared (IR) lamp powered conveyor belt furnaces is well established in the market. The purpose of the project FEUERDRACHE is to advance the classic firing process by raising throughput, energy efficiency and process control via increasing the process variability. To achieve the latter, an industry-oriented furnace is expanded by innovative features, which are thoroughly investigated: 1) faster belt velocity; 2) novel IR lamps; 3) thermography as an inline-capable alternative to thermocouple measurements 4) high-power laser as an alternative to a heated chamber.

MOTIVATION AND AIM

The technology used in passivated emitter and rear cell (PERC) [1] production lines to form the front and rear side contact simultaneously is based on the inline “fast firing equipment” [2]. To heat up the wafers to the needed temperatures of around 780°C to form the contacts, in the complete heating chamber, consisting of a burn-out zone and a peak zone, conventional IR lamps are used. The standard industrial firing furnaces allow only limited variations in the contact firing profile, due to the fact, that the peak zone is held as small as possible with respect to the footprint of the equipment. Furthermore, any integrations of new heat sources are not possible without major changes of the equipment. For temperature measurements - up to now - the method of the thermocouple technique [3] is widely used to profile the process and to control the peak wafer temperature. To do so, an interruption of the cell production is required. There is no inline in-situ measurement technology available to determine the peak temperature of the wafer. The focus of this work is on the evaluation of adapted contact firing processes, development of an alternative firing technology and the setup of an inline measurement system. In this work we present some of the main results that have been achieved during the three-year project “FEUERDRACHE”.

Proceedings of the 9th Workshop on Metallization and Interconnection for Crystalline Silicon Solar Cells
AIP Conf. Proc. 2367, 020004-1–020004-10; https://doi.org/10.1063/5.0056036
Published by AIP Publishing. 978-0-7354-4101-9/$30.00

EQUIPMENT SETUP AND PERC SOLAR CELLS

The base of the investigations is the use of the inline conveyor belt fast firing system by Rehm Thermal Systems located at the PV-TEC laboratory at Fraunhofer ISE. The original equipment is an industrial furnace similar to the ones used in PERC production lines. A scheme of the furnace is shown in Figure 1a. These systems consist of a heating chamber with a burnout phase and a peak phase to perform the contact process, followed by a cooling chamber.

For all cell experiments carried out, passivated PERC pre-cursors from an industrial production line have been used. In order to achieve the goals mentioned in the previous section, the furnace has been enhanced through innovative adaptations and corresponding changes to the equipment. These adaptions are shown in color in Figure 1b and are described in the following. To reach higher throughput, the transport system (changes in green) as well as the peak zone (changes in red) were modified [4]. Compared to a standard furnace, the peak zone, consisting of an upper and lower row of IR lamps, was realized twice (doubled). With the changes in the transport system, a belt velocity of up to 11 m/min can be reached. With this combination, the shape of the profiles in the double peak zone can still be kept constant with high belt velocities, compared to a standard process with lower velocity. To evaluate an alternative firing technology a laser chamber, with laser class 1, right after the heating chamber was set up and a laser system consisting of two VCSEL (vertical cavity emitting surface laser) modules has been integrated (changes in orange) [5]. Furthermore, two positions to realize an optical inspection with an IR camera system have been defined (changes in blue) [6, 7].

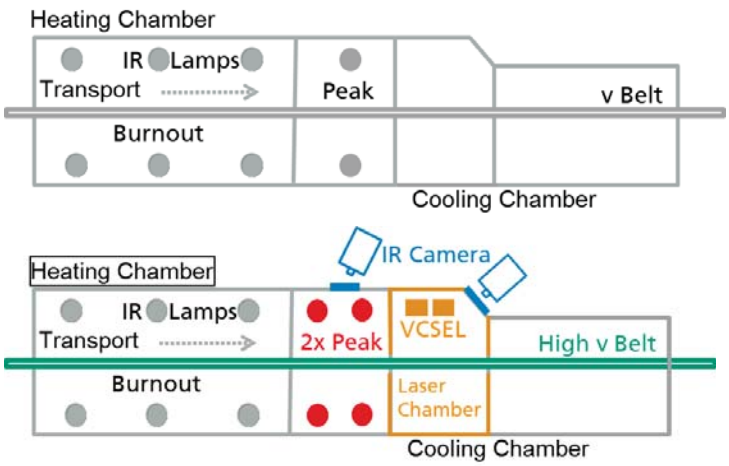

(a) Scheme of a standard industrial fast firing furnace.

(b) Scheme of the industrial oriented fast firing furnace with adaptions marked in color, that were realized to reach the aims of the project.

FIGURE 1. The two figures show the scheme of the fast firing furnace used in the project. (a) shows the original furnace. (b) shows the adapted furnace. In green changes made to realize high belt velocities, in red the ones concerning the peak zone. In orange the adaptions made for the laser firing process are marked and in blue the two possible positions for the integration of the IR camera systems are shown.

The PERC solar cell results shown (based on the pre-cursors), follow a standard process flow, realized in the PV-TEC Back-End laboratory, using a screen printed metallization on the front and rear side, including a regeneration process to suppress the material effect of the boron-oxygen complex [8]. *I-V* measurements were carried out under standard test conditions in the automated inline testing tool.

INVESTIGATION AND RESULTS

In the following four sections the experimental results will be discussed. In the last section a techno-economic investigation will be presented, to show the potential of industrial implementation.

Higher Throughput Realized by Faster Belt Velocities

In the following it is shown, which adaptions have to be made on the firing process, to nearly double the throughput. Starting with a standard belt velocity of 6 m/min (Figure 2a, curve in black), profiles have been created using

thermocouple measurements, reaching a belt velocity of 11 m/min, while keeping the shape of the peak phase identical. Two target profiles with 11 m/min could be realized: in orange one profile with a small burnout plateau and in green one with a steep ramp. The latter is to simulate even higher velocities for which burnout plateaus cannot be realized anymore.

With the two profiles using 11 m/min belt velocity PERC solar cells as described in the experimental setup section, were produced. Figure 2b shows the efficiency values, with a variation of the peak temperature around the optimum for each profile. Exceeding an efficiency level of more than 22%, it could be shown, that there is no difference of the processes with high belt velocities, using the established profiles, compared to the standard process at 6 m/min. With this, the throughput could be increased significantly.

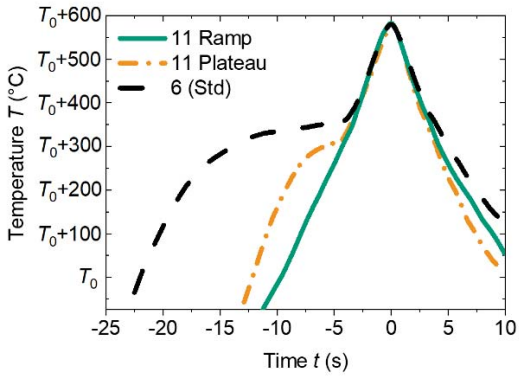

(a) Firing profiles taken with thermocouples.

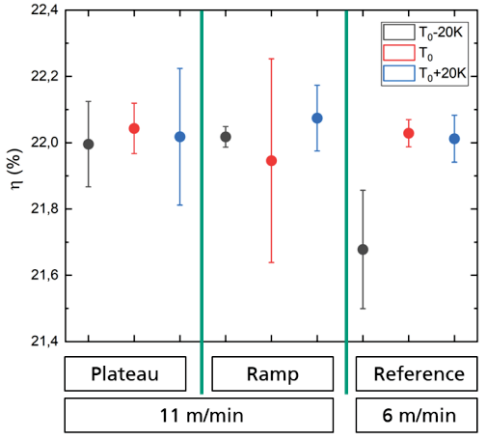

(b) Plot of PERC cell efficiencies, realized with the adapted profiles. T_0 means the peak temperature at the optimum for each profile and T_0 +/-20 the variation of the peak temperature in Kelvin.

FIGURE 2. (a) profiles with different belt velocities taken with thermocouples are displayed. The shape of the peak phase is kept identical for each profile. Standard process with 6 m/min (in black) up to 11 m/min belt velocity. In orange with a small burnout plateau and in green with a steep ramp. (b) the corresponding PERC solar cell efficiencies with two variations around the peak temperature.

To verify, whether the front side fingers of the cells, produced with high belt velocities, are capable to be interconnected with a standard industrial stringer, a module of three cells was produced. For the production of the string, the same parameters for interconnection were used, as for standard cells.

Investigation of Alternative IR Lamps in the Peak Zone

The standard setup of IR lamps, used in the industry in the peak zone are tungsten lamps, normally produced in a double quartz tube shape and mounted perpendicular to the transport direction. The investigations carried out, include the mounting arrangement of the lamps (see Figure 3a left), a filament material of carbon and a coating of the quartz tubes with a reflective material. The latter was coated only on one side of the double quartz tubes and the mounting position was chosen in a way, that a maximum of reflected radiation is directed to the passing wafers. The wavelength peak at maximum power level of the near infrared (NIR) lamps with tungsten filament material is around 1 µm, whereas the peak of the used lamps with carbon material (see Figure 3b) is at around 2.5 µm. All four possible variations compared to the standard setup, horizontally mounted with and without reflecting material for both types of the filament, have been made.

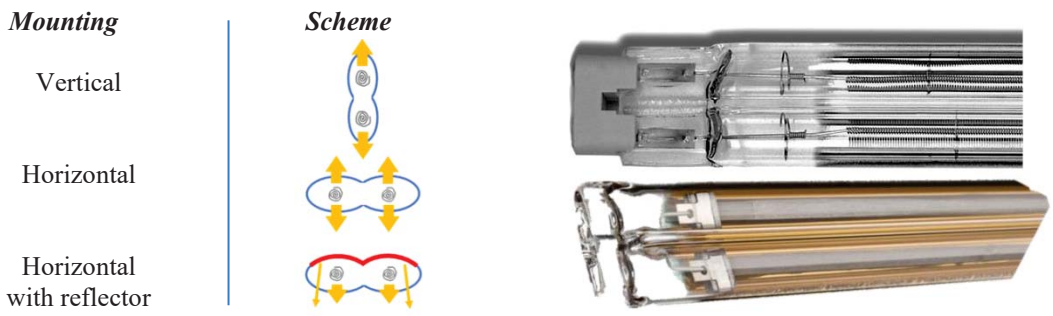

(a) Mounting variations of IR lamps in the peak zone of the furnace.

(b) Images of a double quartz (from Heraeus Noblelight)

FIGURE 3. (a) schematic illustration of double quartz tube lamps used, with and without reflecting material on the quartz tube (red) and the two possible mounting direction (vertical and horizontal). (b) the images show lamps with tungsten (top) and a carbon (bottom) filament material.

PERC solar cells were produced, using the different lamp setups (see Figure 4a on the bottom) and using two different velocities for the different scenarios. The power consumption of the peak zone was measured. The outcome is shown in Figure 4b. The lower power consumption for the lower belt velocity is most likely due to the lower energy dissipation from the peak zone chamber, condemned by the belt and due to the fact that the wafers have more time to heat up. Furthermore, there is no clear trend detectable when using quartz tubes with reflector material, neither for the efficiency nor for the power consumption.

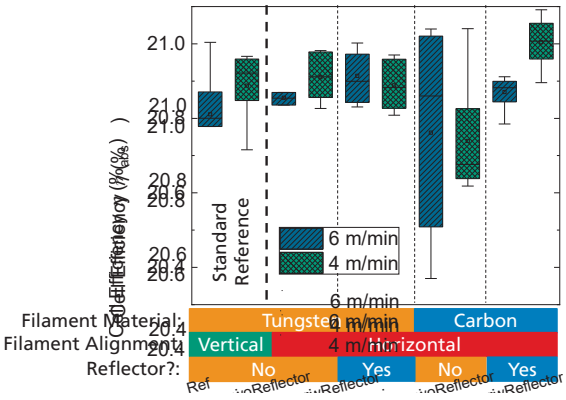

(a) Plot of cell efficiencies for mono-facial PERC cells.

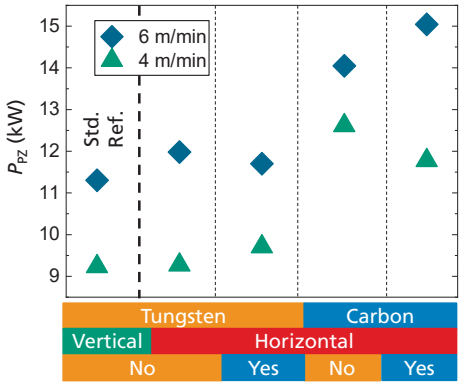

(b) Power consumption of double quartz tube lamps in the peak zone (P_{PZ}).

FIGURE 4. Investigation of alternative IR lamps in the furnace peak zone (PZ) realized through different filament material, reflectors and its alignment. (a) Efficiency of produced PERC cells using different filament material and alignment. (b) The measured output powerof the lamps used in the peak zone during processing with the different setups.

The results obtained do not constitute a recommendation to use a different combination compared to the standard lamps and their design.

Establishment of a Spatially Resolved Quality Assurance via IR Camera System

The need to profile an inline heating furnace in terms of temperature distribution is obvious. The main method to do so, is the use of thermocouples with a data logging system. Therefore, the production has to be interrupted and it can only be done for a single wafer. The most important part of the firing profile, when looking at the contact formation, is the wafer peak temperature. This section will present the high-end IR camera systems from InfraTec (ImageIR 8300) [9] integrated into two positions in the fast firing equipment, to measure the peak temperature of the

wafers. In Figure 1b the positions are marked in blue. One is in the last part of peak zone for the use of the classic firing process and the second is to observe the peak temperature while the laser firing process takes place. In both cases an isolating window is integrated to generate an optical path, isolate the surroundings in terms of heat or laser radiation. For both setups a temperature correction has to be performed. To create an optical path into the heat chamber, the isolation of the chamber has to be partly opened. A sketch of the optical path can be seen in Figure 5a on the bottom. Opening the isolation wall of a heated furnace is crucial. Therefore, thermocouple measurements have been taken before and after the creation to check, whether a difference can be detected, but this was not the case. Figure 5a (top) shows a snapshot of the trailing part of the wafer taken with the IR camera system. The red dotted line marks the section of the camera field of view, limited by the implemented optical channel. The last top IR lamp is visible within the view. The transport belt can be seen on the left and right side. To get a 2D spatially resolved temperature mapping, an analyzing script to extract the peak temperature from the passing wafers is created. On the top of Figure 5b [5], such a 2D mapping is shown. The results from the analysis of these mappings are displayed on the bottom. Perpendicular to the transport direction, optical effects can be seen at the positions of the busbars. The drop of the temperature at the edges of the wafers, can be explained because of a heat dissipation from the slightly lower temperature of the surroundings and the air flow within the chamber. Analyzing the temperature distribution in transport direction, the graph on the bottom right shows that the heading part of the wafer has a lower temperature than the trailing part. This is due to the fact, that as long as the wafer is not heated up once, a temperature diffusion from the heated part to the trailing part of the wafer takes place. Nevertheless, a peak temperature distribution of around +/-5K can be reached.

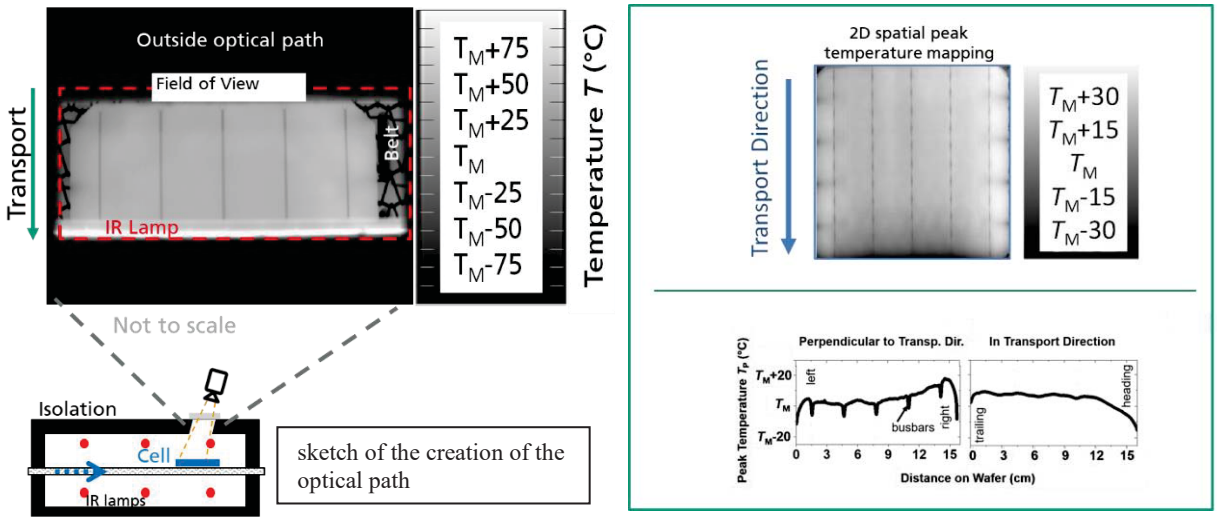

(a) Snapshot of the trailing part of the wafer, while passing the peak zone of the heated firing chamber.

(b) 2D spatial mapping of the peak temperature taking by the ImageIR 8300 camera system from InfraTec.

FIGURE 5. T_M meaning the mean temperature over the complete wafer. (a) Snapshot with temperature scale taken by the IR camera system from a wafer passing the peak zone of the heated chamber. (b) 2D spatial mapping of the peak temperature of a wafer, derived from an analyzing script (top). Temperature distribution perpendicular (left) and in transport (right) direction.

Evaluation of Alternative Firing Process by VCSEL Technology

Until now there is no alternative for the firing process technology available, being inline suitable and capable for high throughput. The alternative of a RTP-process [10] IR lamps were used to heat up the wafer and therefore it is the same technology than used in the industry but not applicable in mass production. With the VCSEL technology by TRUMPF Photonics (former Philips Photonics) an alternative technology is introduced for the fast firing process. Through the integration of two ~5 kW modules between the heating and cooling chamber (Figure 1b in orange and Figure 6a), we could investigate the potential of this technology. The two modules are mounted perpendicularly to the transport direction with the laser area facing towards the belt. In order to have the possibility to keep the overlap of

the two laser areas of the modules, which are directed on the wafer, flexible, the construction was realized in such a way, that the modules can be tilted horizontally. Each module (see Figure 6a zoom) consists of 24 segments. These segments can be independently powered, have a very short response time and hence spatial and temporal profiles can be realized.

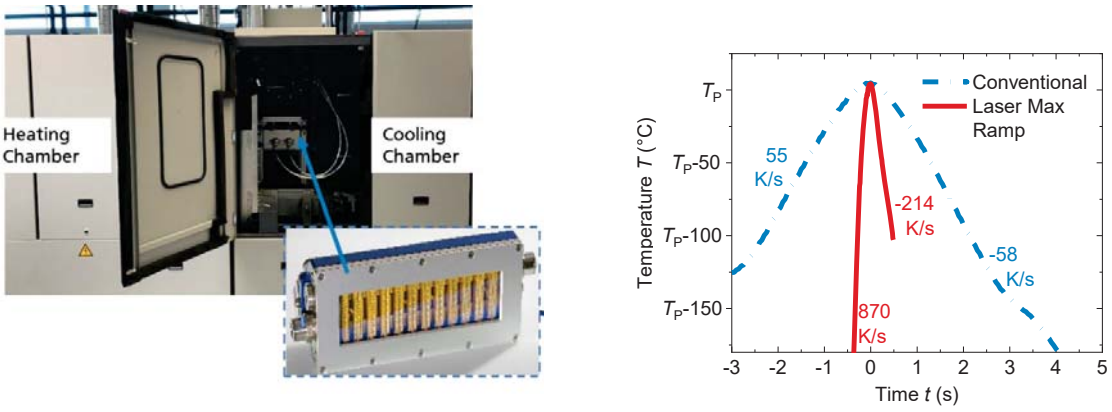

(a) Integration of two VCSEL modules in the fast firing furnace.

(b) Profiles taken with thermocouples.

FIGURE 6. (a) Integration of the VCSEL modules in the fast firing equipment to realize an alternative peak zone for the firing process. The beam of the laser modules are directed towards the belt. The modules can be tilted and adapted in height. Two mirrors are placed parallel to the transport direction (not shown) to homogenize the temperature profile. (b) Representative possible profiles taken with thermocouples on PERC solar cells. In blue with the conventional firing process and in red with the VCSEL modules.

As can be seen from Figure 6b the heating and cooling ramps, that can be realized with the VCSEL modules in this setup are significantly steeper. For the solar cell processing however, the shape of the peak was kept identical to the classic firing process. A big effort was invested in realizing a great degree of temperature homogeneity on the wafer, but still there is potential for an optimization in the setup and thus in the homogeneity, especially perpendicular to the transport direction.

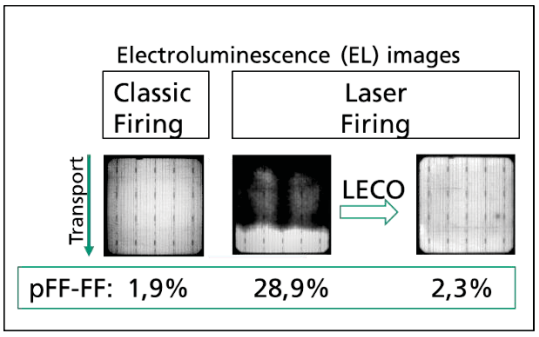

(a) EL images for PERC solar cells with the value *pFF-FF* underneath, represent the series resistance.

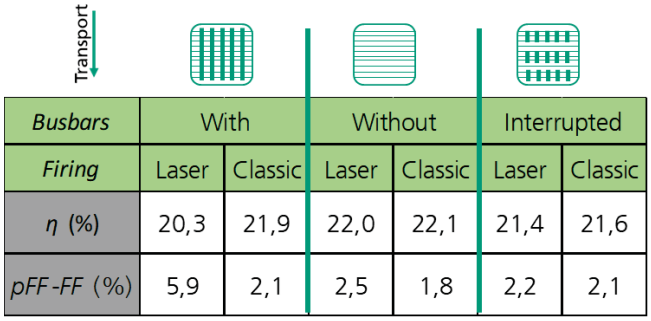

Busbars	With		Without		Interrupted	
Firing	Laser	Classic	Laser	Classic	Laser	Classic
η (%)	20,3	21,9	22,0	22,1	21,4	21,6
pFF-FF (%)	5,9	2,1	2,5	1,8	2,2	2,1

(b) PERC solar cell fired by laser and conventionally. The efficiencies and the *pFF-FF)* value are shown.

FIGURE 7. (a) EL images of p-type mono-facial PERC solar cells with H-grid front side pattern are shown. Left with classic firing process, in the middle direct after laser firing and right after laser firing and applying the LECO process to heal the underfired parts of the front side metallization. The corresponding value of *pFF-FF* is displayed underneath. (b) Comparison of solar cell efficiencies and the value *pFF-FF* (representing the series resistance) for different front side metallization patterns (shown on top in green), fired with both technologies.

While processing with the laser firing technology, one effect is that the surrounding of the process area stays at fairly low temperature. This means that the main heat transfer to the wafer comes directly from the laser radiation, whereas in the classic firing situation, it is a combination of direct and indirect (reflected) radiation and from

convection through the heated up atmosphere. Due to the fact, that the process area in transport direction is smaller than the length of the wafer, at a certain point of time, a temperature inhomogeneity in transport direction is inevitable. If a standard H-grid front side metallization is used, the appearance of the "short circuit effect" (SC-effect) introduced by Kim *et al.* [11] is most likely. The effect is especially apparent in the series resistance, made visible in the EL image (Figure 7a middle) and of the resistive losses represented by the *pFF-FF* values. Within the project, we investigated three different possibilities to deal with this effect. Because the SC effect leads to partially underfired contacts, the LECO [12] process can be used to heal these areas. As it can be seen, in the EL image and in the corresponding value representing the series resistance in Figure 7a, the same contact quality can be achieved, when applying the LECO process on cells with high series resistances. To prevent the SC-effect from affecting the performance of the solar cell, areas on the cell that have a temperature difference at a certain time point, must not be connected by the metallization on the front side. This was demonstrated by Chu *et al.* [13] using a front side metallization pattern without busbars and processing the cells with front side fingers perpendicularly aligned to the transport direction, the suspected effect becomes negligible. In this case, the efficiencies of the cells are only $0.1\%_{abs}$ lower than the ones fired with the classic technology. The third possibility is the use of an interrupted busbar front side pattern (scheme on Figure 7b top right). In this case the same *pFF-FF* value of 2.2% compared to the reference process is reached. The main advantage of the interrupted busbar design, compared to the busbar-less pattern, is the possible use of a standard interconnection to produce strings for module interconnection.

Cost of Ownership Investigation of the Firing Technologies, Process and Integration of the IR Camera System

Besides the experimental investigations, shown in the previous sections, in the following the Cost of Ownership (COO) will be discussed. The Fh-ISE uses the in-house developed and cost accounting model "SCost" [14, 15] to evaluate the production costs or COO of manufacturing processes in industrial PV production. The model is based on the SEMI standards E35 and E10 [16–18], which are established in the PV industry. For all following calculations, a dual line setup of the fast firing equipment was taken into account.

Figure 8a shows the effect on the COO of accomplishing a higher throughput, using a higher belt velocity, in €ct/Wp. It can be seen the costs are nearly halved, with the fixed equipment costs staying constant and the recurring costs only rising little, if the throughput is doubled. Looking at the integration of a high-end IR camera system (in this case ImageIR 8300 from InfraTec) to realize a quality assurance by tracking the peak temperature of every cell produced and assuming that the shape of the efficiency distribution could be sharpened leading to an average production efficiency of $0.1\%_{abs}$., the COO for the additional camera invest are already almost compensated when looking at the firing step alone. But it is to note that a cell efficiency increase benefits all area related costs along the PV value chain [14]. Thus, the advantage one gets through tracking the peak temperature of each wafer can exceed the additional required investment in the camera system, if this results in an average production efficiency advantage.

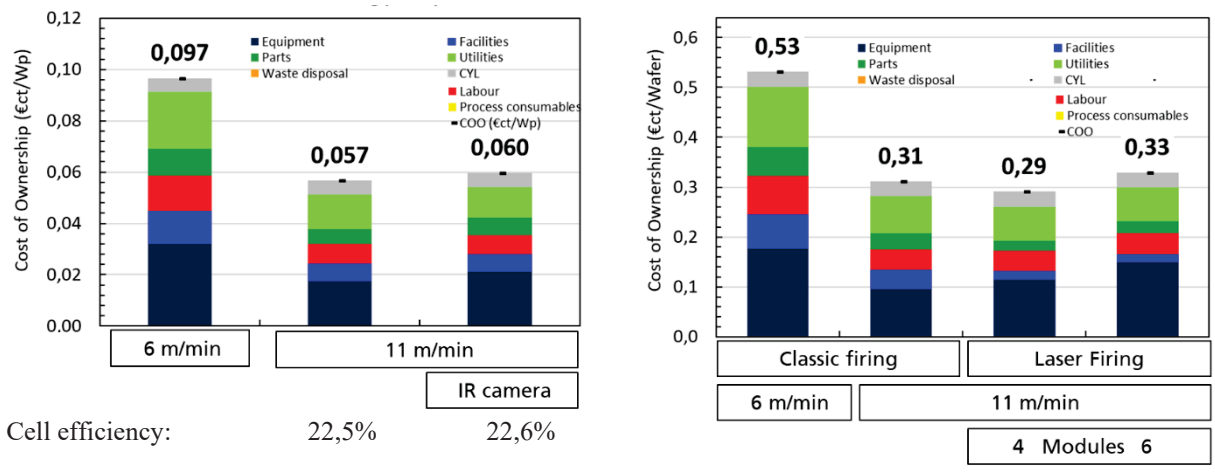

(a) COO investigation in €ct/Wp.

(b) Comparison of the COO in €ct/wafer

FIGURE 8. COO investigation with the *Fh-ISE SCost* model for (a) a higher throughput by increasing the belt velocity from 6 m/min to 11 m/min and the integration of a high-end IR camera system into a firing furnace and for (b) the alternative firing compared to the classic process. For the faster process of 11 m/min 4 or 6 modules are taken into account.

To see whether the alternative firing technology with VCSEL modules are compatible in terms of cost per wafer, the process costs were calculated with a transport velocity of 11 m/min. As the process is still in a phase of optimization, two possibilities have been considered. As the classic furnace in industry is mostly a dual lane equipment, this was retained in the design with the VCSEL technology. Hence, for one "firing lane" a setup with two or three modules – meaning four or six modules in total – has been calculated. The COO results is shown in Figure 8b on the right. For an implementation with only two modules per lane, the COO in €ct/wafer result in a slight decrease (-0.02 €ct/wafer), and with three modules per lane in a slight increase (+0.02 €ct/wafer), in comparison to the classic firing reference at 11 m/min. Whereas the CAPEX requirement of the Laser Firing is higher as for the Classic Firing system, the area requirement decreases and the maintenance costs are expected to be lower, being able to compensate the increased investment during operation. However, we have to note, that these small differences in COO are lower than the uncertainties with the implementation of a new production technology. Nevertheless, the COO results show the potential of this new technology.

Summary and Outlook

Within the project "FEUERDRACHE" we could achieve an advanced conventional firing process with higher throughput and same efficiencies compared to the standard process. This was made possible by adapting the peak zone and hence being able to realize identical peak profiles. The investigation on the alternative lamps, by changing the mounting setup, filament material and using reflective material, has shown, that these changes are not beneficial, which is a valuable feedback to lamp and furnace manufacturers. We were able to prove that the IR thermography technology can be used in both classical and laser firing processes to realize a contact-less, spatially resolved and cost-neutral inline measuring system, for quality assurance for each wafer produced. Furthermore, for the first time, we could establish an alternative firing process based on laser technology using VCSEL modules on PERC solar cells. The COO investigation on the integration of an IR camera inspection system and on the laser firing technology shows the potential of implementation into a mass production line.

In the future, we will investigate on even faster firing processes for both technologies. With the data taken by the IR camera system, we want to do a correlation of the real wafer peak temperature to the solar cell *I-V* measurement parameters, to get an even deeper insight on the contacting process. An "on-the-fly" adaption of the peak temperature, resulting from changes in earlier process steps, is especially imaginable with the laser firing technology. With the latter, a process development on the TOPCon cell technology is obvious. To establish a complete alternative firing technology, an alternative heating technology for the burnout zones will be investigated.

ACKNOWLEDGMENTS

This work was supported by the German Federal Ministry for Economic Affairs within the research project "FEUERDRACHE" (0324205A & 0324205B). The authors thank the project partners *InfraTec*, *Rehm Thermal Systems*, *Heraeus Noblelight* and *Trump Photonic Components* for co-financing and support as well as all the co-workers who contributed to this investigation. For processing the solar cells with the LECO process, we thank CE CELL ENGINEERING GMBH.

REFERENCES

[1] A. W. Blakers, A. Wang, A. M. Milne, J. Zhao, and M. A. Green, "22.8% efficient silicon solar cell," *Appl. Phys. Lett.*, vol. 55, no. 13, pp. 1363–1365, 1989, doi: 10.1063/1.101596.

[2] J. Xu, J.Zhang, K.Kuang, *Conveyor Belt Furnace Thermal Processing*. Heidelberg: Springer, 2018.

[3] L. Michalski, K. Eckersdorf, J. Kucharski, J. McGhee, *Temperature Measurement: Second Edition*. West Sussex, England: John Wiley & Sons, Ltd, 2001.

[4] D. Ourinson, G. Emanuel, A. Lorenz, F. Clement, and S. W. Glunz, "Evaluation of the burnout phase of the contact firing process for industrial PERC," *AIP Conference Proceedings*, p. 40015, 2019, doi: 10.1063/1.5123842.

[5] D. Ourinson, G. Emanuel, K. Rahmanpour, F. Ogiewa, H. Müller, E. Krassowski, H. Höffler, F. Clement, S. W. Glunz, "Laser-Powered Co-Firing Process for High-Efficient Si Solar Cells: Submitted," 2020.

[6] D. Ourinson *et al.,* "In Situ Solar Wafer Temperature Measurement during Firing Process via Inline IR Thermography," *Phys. Status Solidi RRL*, p. 1900270, 2019, doi: 10.1002/pssr.201900270.

[7] D. Ourinson, G. Emanuel, G. Dammaß, H. Müller, F. Clement, and S. W. Glunz, "In Situ Surface Temperature Measurement in a Conveyor Belt Furnace via Inline Infrared Thermography," *Journal of visualized experiments : JoVE*, no. 159, 2020, doi: 10.3791/60963.

[8] T. Niewelt, J. Schön, W. Warta, S. W. Glunz, and M. C. Schubert, "Degradation of Crystalline Silicon Due to Boron–Oxygen Defects," *IEEE J. Photovoltaics*, vol. 7, no. 1, pp. 383–398, 2017, doi: 10.1109/JPHOTOV.2016.2614119.

[9] *Infratec.* [Online]. Available: https://www.infratec.de/thermografie/waermebildkameras/imageir-8300/ (accessed: Apr. 1 2019).

[10] D. M. Huljic, G. Grupp, R. Preu, and J. Horzel, "Comprehensive study of rapid thermal firing for industrial production of crystalline silicon thick-film solar cells," in *19th EU PVSEC*, Paris, 2004, pp. 580–583.

[11] H.-S. Kim *et al.,* "Electrochemical nature of contact firing reactions for screen-printed silicon solar cells: origin of "gray finger" phenomenon," *Prog. Photovolt: Res. Appl.*, vol. 24, no. 9, pp. 1237–1250, 2016, doi: 10.1002/pip.2783.

[12] E. Krassowski, S. Großer, M. Turek, and H. Höffler, "Laser Enhanced Contact Optimization – A Novel Technology for Metal-Semiconductor-Contact Optimization for Crystalline Silicon Solar Cells," *37th Photovoltaic Conference Proceedings, Online-Conference*, 2020.

[13] H. Chu *et al.,* "Impact of the Presence of Busbars During the Fast Firing Process on Contact Resistances," *IEEE J. Photovoltaics*, vol. 8, no. 4, pp. 923–929, 2018, doi: 10.1109/JPHOTOV.2018.2828824.

[14] S. Nold *et al.,* "Cost Modeling of Silicon Solar Cell Production Innovation along the PV Value Chain," in *27th EU PVSEC*, Frankfurt, 2012, pp. 1084–1090.
[15] S. Nold, *Techno-ökonomische Bewertung neuer Produktionstechnologien entlang der Photovoltaik-Wertschöpfungskette: Modell zur Analyse der Total Cost of Ownership von Photovoltaik-Technologien*. Stuttgart: Fraunhofer Verlag, 2020. [Online]. Available: http://publica.fraunhofer.de/documents/N-574724.html
[16] *Specification for Definition and Measurement of Equipment Productivity*, E79-0814, 2014.
[17] *Specification for Definition and Measurement of Equipment Reliability, Availability, and Maintainability (RAM)*, E10-0814E, 2014.
[18] *Guide to calculate Cost of Ownership (COO) metrics for semiconductor manufacturing equipment*, E35-0618, 2018.